THE JOURNAL OF BIOLOGICAL CHEMISTRY VOL. 291, NO. 19, pp. 9920–9928, May 6, 2016

Cathepsin S Contributes to the Pathogenesis of Muscular Dystrophy in Mice*

Received for publication, February 4, 2016, and in revised form, March 10, 2016 Published, JBC Papers in Press, March 10, 2016, DOI 10.1074/jbc.M116.719054

Andoria Tjondrokoesoemo[‡], Tobias G. Schips[‡1], Michelle A. Sargent[‡], Davy Vanhoutte[‡], Onur Kanisicak[‡2], Vikram Prasad[‡], Suh-Chin J. Lin[‡], Marjorie Maillet[‡], and Jeffery D. Molkentin[‡§3]

From the [‡]Department of Pediatrics and [§]Howard Hughes Medical Institute, Cincinnati Children's Hospital Medical Center, University of Cincinnati, Cincinnati, Ohio 45229

Duchenne muscular dystrophy (DMD) is an X-linked recessive disease caused by mutations in the gene encoding dystrophin. Loss of dystrophin protein compromises the stability of the sarcolemma membrane surrounding each muscle cell fiber, leading to membrane ruptures and leakiness that induces myofiber necrosis, a subsequent inflammatory response, and progressive tissue fibrosis with loss of functional capacity. Cathepsin S (Ctss) is a cysteine protease that is actively secreted in areas of tissue injury and ongoing inflammation, where it participates in extracellular matrix remodeling and healing. Here we show significant induction of Ctss expression and proteolytic activity following acute muscle injury or in muscle from *mdx* mice, a model of DMD. To examine the functional ramifications associated with greater Ctss expression, the *Ctss* gene was deleted in the *mdx* genetic background, resulting in protection from muscular dystrophy pathogenesis that included reduced myofiber turnover and histopathology, reduced fibrosis, and improved running capacity. Mechanistically, deletion of the *Ctss* gene in the *mdx* background significantly increased myofiber sarcolemmal membrane stability with greater expression and membrane localization of utrophin, integrins, and β-dystroglycan, which anchor the membrane to the basal lamina and underlying cytoskeletal proteins. Consistent with these results, skeletal muscle-specific transgenic mice overexpressing Ctss showed increased myofiber necrosis, muscle histopathology, and a functional deficit reminiscent of muscular dystrophy. Hence, Ctss induction during muscular dystrophy is a pathologic event that partially underlies disease pathogenesis, and its inhibition might serve as a new therapeutic strategy in DMD.

Duchenne muscular dystrophy (DMD)[4] is an X-linked inherited neuromuscular disease because of mutations in the gene encoding dystrophin, which affects 1 in 5000 males (1). DMD pathogenesis is characterized by the appearance of muscle weakness and fatigue in juveniles that progresses to muscle-based paralysis in young adult patients, with eventual death because of respiratory failure or cardiomyopathy (2, 3). Dystrophin is a component of the membrane-anchored dystrophin-glycoprotein complex, whose primary function is to anchor the intracellular cytoskeleton to the extracellular matrix (ECM), thus providing structural support to the sarcolemma (4, 5). Loss of dystrophin protein results in destabilization of the greater dystrophin-glycoprotein complex and sarcolemmal fragility that leads to the unrestrained influx of calcium, causing myofiber necrosis and the induction of tissue inflammation, fibrosis, and a progressive loss of muscle contractile performance (4, 5). Currently there is no cure for DMD, and although gene therapy to restore dystrophin expression is a promising concept, it remains in the distant future (6). Thus, it will be critical to develop novel pharmacologic therapies that address key aspects of disease pathogenesis, such as increased protease activity (7, 8).

Cathepsin S (Ctss) belongs to the family of lysosomal cysteine proteases. Ctss was first identified in macrophages and dendritic cells as a major endoprotease cleaving the invariant chain from the major histocompatibility class II complex prior to antigen presentation (9–11). Genetic deletion of the *Ctss* gene in the mouse does not affect viability, although these animals have altered antigen processing that causes a mild immune-compromised phenotype (9). In addition to its role in antigen processing, Ctss can remodel the ECM in various tissues when secreted. Unlike others acidic lysosomal proteases, Ctss remains catalytically active and stable in a neutral pH environment, allowing for its proteolytic activity when secreted. Collagen, elastin, and fibronectin are some of the ECM proteins cleaved by Ctss (12, 13).

Numerous studies have demonstrated that increased activity of select proteases in the skeletal muscle of mouse models of muscular dystrophy, such as the calpains and matrix metalloproteinases, contributes to tissue histopathology (7, 14). For example, genetic inhibition of a broad class of serine proteases achieved by overexpressing the inhibitor Serpina3n in skeletal muscle attenuated dystrophic disease in two mouse models of muscular dystrophy (15). Furthermore, skeletal muscle func-

* This work was supported by National Institutes of Health Grant P01NS072027 (to J. D. M.) and a grant from the Howard Hughes Medical Institute (to J. D. M.). The authors declare that they have no conflicts of interest with the contents of this article. The content is solely the responsibility of the authors and does not necessarily represent the official views of the National Institutes of Health.

[1] Supported by German Research Foundation Grant SCHI 1290/1-1).

[2] Supported by Postdoctoral Fellowship 15POST25480009 from the American Heart Association.

[3] To whom correspondence should be addressed: Cincinnati Children's Hospital Medical Center, 240 Albert Sabin Way, MLC7020, Cincinnati, OH 45229. Tel.: 513-636-3557; Fax: 513-636-5958; E-mail: jeff.molkentin@cchmc.org.

[4] The abbreviations used are: DMD, Duchenne muscular dystrophy; ECM, extracellular matrix; Ctss, Cathepsin S; Tg, transgenic; NTG, non-transgenic; $BaCl_2$, barium chloride; EBD, Evans blue dye; TA, tibialis anterior; CK, creatine kinase; LHVS, *N*-morpholinourea-leucine-homophenylalanine-vinyl-sulfonephenol.

tion in various muscular dystrophy models was improved following application of broad serine protease inhibitors or antifibrotic drugs known to modulate matrix metalloproteinase activity (14, 16). Such studies led us to examine proteases that are both induced in dystrophic skeletal muscle and amenable to pharmacologic inhibition, which might represent a new therapeutic approach in DMD. One of these proteases, Ctss, was previously identified as an mRNA species up-regulated in both muscle from DMD patients and *mdx* mice, although the functional effects of this increase were not investigated (17–19).

Here we observed that Ctss expression and activity are up-regulated in the skeletal muscle of *mdx* mice. Deletion of the *Ctss* gene in the *mdx* background resulted in healthier skeletal muscle with reduced myofiber degeneration and fibrosis and improved running performance. Mechanistically, loss of Ctss in *mdx* mice stabilized membrane adhesion complexes and levels of associated proteins, such as utrophin, β-dystroglycan, and the integrins, thereby increasing sarcolemma membrane stability and protection from injury. We also generated a skeletal muscle-specific transgenic mouse overexpressing Ctss (Ctss TG). These mice had greater muscle Ctss proteolytic activity that was associated with induction of muscle histopathology reminiscent of muscular dystrophy. Hence, increased Ctss expression and activity in skeletal muscle is detrimental to DMD pathology, and its inhibition represents a novel therapeutic vantage point for this disease.

Experimental Procedures

Animals—All animal procedures were approved by the Institutional Animal Care and Use Committee of the Cincinnati Children's Hospital Medical Center (protocol IACUC2013-0013). The exact number of mice used is given in the figure legends or within the figures, and the numbers used reflect the minimum needed to achieve statistical significance (see "Statistics"). Animals used in the study were not randomized or handled in a blinded manner because this was not commensurate with the experimental design. No data collected from animals were excluded. No human subjects were used. *Ctss*$^{-/-}$ mice were provided by Dr. Guo-Ping Shi (9). *mdx* mice were obtained from The Jackson Laboratory (stock no. 001801). To generate *mdx/Ctss*$^{-/-}$ mice, *mdx* female mice in the C57Bl/10 background were mated with male *Ctss*$^{-/-}$ mice in the related C57Bl/6 background. The subsequent litters were backcrossed three times to generate *mdx/Ctss*$^{-/-}$ mice, and only male *mdx/Ctss*$^{-/-}$ and *mdx* littermates were used. WT C57Bl/6 male mice were used as controls. The following primers were used for *Ctss*$^{-/-}$ genotyping: Neo cassette (forward, 5′TGA ATG AAC TGC AGG ACG AG; reverse, 5′AAT ATC ACG GGT AGC CAA CG), WT (forward, 5′CTC TGT GTA GCC TGG AAT TCA C; reverse, 5′ATG CCA GAT GCA AAA AGC TTT AAC), and KO (forward, same primer as the WT forward sequence; reverse, 5′ACT TGT GTA GCG CCA AGT GCC). Genotyping for *mdx* was performed as shown previously (20).

The mouse Ctss cDNA was cloned in a modified human skeletal α-actin promoter (21) to create skeletal muscle-specific TG mice (FVBN strain). Two TG lines were generated by DNA injection into newly fertilized mouse oocytes. TG males were compared with NTG littermate males. The following primers were used for genotyping of the Ctss transgene: forward, 5′CGA GAG TAG CAG TTG TAG CTA; reverse, 5′CAC AGT GTC AGG CAA TGT CC.

Protease Activity Assay—A Ctss activity assay (Abcam, ab65307) was used to measure the cysteine proteolytic activity in either the dystrophic or $BaCl_2$-injured skeletal muscle. Other cysteine protease activities measured included cathepsin B (Abcam, ab65300) and cathepsin L (Abcam, ab65306). Briefly, isolated muscles were frozen, ground into a fine powder using a mortar and pestle, and sonicated before the ice-cold buffer from the assay kit was added to the samples. The enzymatic assay itself was conducted according to the instructions of the manufacturer.

Western Blotting and Protein Extraction from Skeletal Muscle—Isolated muscles were frozen and ground to a fine powder using a mortar and pestle, homogenized, sonicated, and then added to ice-cold radioimmune precipitation assay buffer. Ctss was detected using rabbit polyclonal antibody from EMD Millipore (catalog no. 219384, 1:1000, against human and mouse epitope) by Western blotting as described previously (15).

Skeletal muscle membrane enrichment protein fractions were prepared following a protocol described previously (22). Standard Western blotting was then performed with the membrane-enriched protein extracts as shown previously (15). Primary antibodies used were α5-integrin (EMD Millipore, AB1928, 1:1000, polyclonal rabbit against mouse). The other antibodies used are listed in a study published previously (15).

ECM protein fractionation from quadriceps muscle was generated as described previously (23). Primary antibodies used included collagen IV (Abcam, ab19808, 1:1000, rabbit polyclonal against mouse) and fibronectin (Abcam, ab2413, 1:1000, rabbit polyclonal against mouse). These extracts were then subjected to Western blotting as described previously (15).

RNA Expression Analysis—Total RNA was extracted from muscles using the RNeasy kit according to the instructions of the manufacturer (Qiagen) and reverse-transcribed using SuperScript® III reverse transcriptase (Invitrogen, 18080-044). Differences in transcript levels were analyzed by real-time quantitative PCR using SYBR Green (Applied Biosystems). The primer sequences for Ctss were as follows: forward, 5′TGC GTC ACT GAG GTG AAA TAC C; reverse, 5′ CTT CAT TTG AGC AGT CCA CCA G. The primer sequences for other genes are listed in a previous study (15).

Histological Analysis and Immunohistochemistry—Muscles were paraffin-embedded, and 6-μm histological sections were cut at the center of the muscle and stained with H&E or Masson trichrome. Pictures were generated at a magnification of ×200, and fibers of the quadriceps muscle were counted for central nucleation using ImageJ software (National Institutes of Health). Interstitial fibrotic regions were quantified using MetaMorph 7.1 (Molecular Devices) as the percentage of the blue area stained with Masson trichrome. Immunohistochemistry was performed on muscle histological cryosections from optimal cutting temperature compound-embedded muscles using the following antibodies: Ctss (Abcam, ab96788, 1:100, rabbit polyclonal against human epitope), Laminin α-2 chain (Sigma-Aldrich, L0663, 1:200, rat monoclonal against mouse and human), and lysosome-associated membrane protein 2

(Lamp-2, Abcam, ab13524, 1:100, rat monoclonal against mouse and rabbit). Nuclei were stained blue with 1 mg/ml DAPI diluted to 1:5000 in saline. Wheat germ agglutinin-FITC (Sigma-Aldrich, L4895) was used at 50 μg/ml to outline membranes in Evans blue dye (EBD) experiments. Antibodies used for immunohistochemistry of sarcolemma adhesion components were described previously (15).

EBD Uptake and Involuntary Running—Mice were injected with Evans blue dye (intraperitoneally, 10 mg/ml, 0.1 ml/10 g of body weight). Twenty-four hours later, mice were subjected to forced treadmill running for 30 min and sacrificed. The tibialis anterior (TA) muscles were removed, embedded in optimal cutting temperature compound and snap-frozen in liquid nitrogen as described previously (15). For the treadmill running protocol, ~2- to 4-month-old mice were acclimatized to the treadmill (Omni-Pacer LC4/M, Columbus Instruments International) for 10 min at a speed of 6 m/min prior to shock grid activation. The speed was then changed to 10 m/min for 30 min. Running capacity was assessed by the maximum running endurance time before exhaustion. Exhaustion was determined by the animal remaining on the shock grid for more than 10 consecutive seconds.

$BaCl_2$ Injury—Sixty microliters of an aqueous 1.2% mass/volume $BaCl_2$ (Sigma-Aldrich, 202-7385g) solution was injected along the whole length of the left TA muscle to induce injury and degeneration (24).

Enzymatic Dissociation of Myofibers and Laser Sarcolemma Membrane Stimulation—Myofiber isolation from the flexor digitorum brevis was performed as described previously (15). Enzymatically dissociated flexor digitorum brevis fibers were plated onto Mattek glass-bottomed dishes containing 1.25 mM Ca^{2+} isotonic Tyrode solution. Damage to the myofibers was induced by irradiating a 5 × 5 pixel area on the sarcolemma membrane with 80 milliwatts at 351/364-nm wavelength for 10 s using a Nikon A1 confocal microscope equipped with a ×60 water immersion lens in the presence of 2.5 μM FM1-43 dye (Molecular Probes) in the extracellular Tyrode solution. Images were captured at 5-s intervals following irradiation with the laser. The mean fluorescence intensity in the damaged area was quantified by ImageJ software. Calcium-free analysis was performed by replacing the 1.25 mM Ca^{2+} with isotonic Tyrode solution lacking this divalent cation, which was also supplemented with 0.5 mM EGTA.

Statistics—All results are presented as mean ± S.E. Statistical analysis was performed with unpaired two-tailed *t* test (for two groups) and one-way analysis of variance with Bonferroni correction (for groups of three or more). *p* values of <0.05 were considered significant. Animal numbers reflected the minimal number needed for statistical significance based on power analysis and prior experience. No data were excluded from the animal experiments, and blinding was not performed.

Results

Ctss Is Up-regulated in Injured Skeletal Muscle—mRNA profiling in humans with DMD and the *mdx* mouse showed an increase in Ctss expression (17–19), which we also observed in Affymetrix arrays from the muscle of δ-sarcoglycan-deficient mice ($Sgcd^{-/-}$), a model of limb-girdle muscular dystrophy,

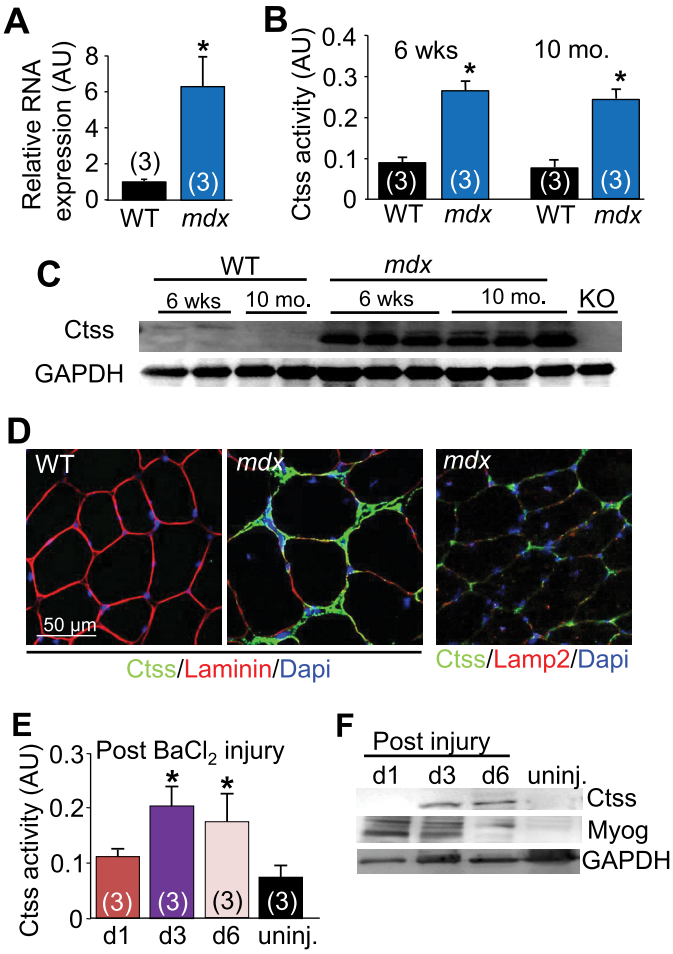

FIGURE 1. **Ctss is expressed in damaged skeletal muscle**. *A*, quantitative PCR for Ctss mRNA measured from the quadriceps of 2- to 3-month-old *mdx* mice compared with the WT. *, $p < 0.05$ *versus* WT. The number of mice analyzed is indicated in the graph. *AU*, arbitrary units. *B*, increased Ctss protease activity in the quadriceps of *mdx* mice compared with WT at 6 weeks (*wks*) and 10 month (*mo*) of age. *, $p < 0.05$ *versus* WT at the same time point. The number of mice analyzed is indicated in the graph. *C*, Western blotting analysis for Ctss expression in the quadriceps of 6-week- and 10 month-old *mdx* mice compared with WT mice of the same age. GAPDH was a processing and loading control. KO represents muscle protein extracts isolated from the quadriceps of $Ctss^{-/-}$ mice as a negative control. *D*, immunohistochemistry from the quadriceps of WT and *mdx* mice for Ctss expression (*green*) *versus* the myofiber outline with laminin (*red*) or the lysosomal marker Lamp2 (*red*). Nuclei are shown in *blue* with DAPI staining. *E* and *F*, Ctss activity assay (*E*) and expression (*F*) in the TA muscle of WT mice on the indicated days (*d*) following acute $BaCl_2$ injection injury or from uninjured (*uninj.*) muscle. Myogenin (*Myog*) was used as a marker for muscle injury, and GAPDH was a processing and loading control. *, $p < 0.05$ *versus* uninjured. All *error bars* show mean ± S.E. The number of mice analyzed in *E* is indicated in the graph.

and in transgenic mice overexpressing the calcium/sodium influx channel Trpc3 that also develop a muscular dystrophy phenotype (25). To validate these prior observations from various gene arrays, we performed quantitative PCR for Ctss, which revealed a 6-fold up-regulation of this mRNA in the skeletal muscle of *mdx* mice (Fig. 1*A*). More importantly, Ctss activity assays and Western blotting from skeletal muscle of *mdx* mice demonstrated Ctss up-regulation, this time at 6 weeks and 10 months of age (Fig. 1, *B* and *C*). Immunohistochemistry showed essentially no Ctss expression (*green*) in normal skeletal muscle, but skeletal muscle from *mdx* mice had abundant Ctss protein co-localized with laminin within the ECM region

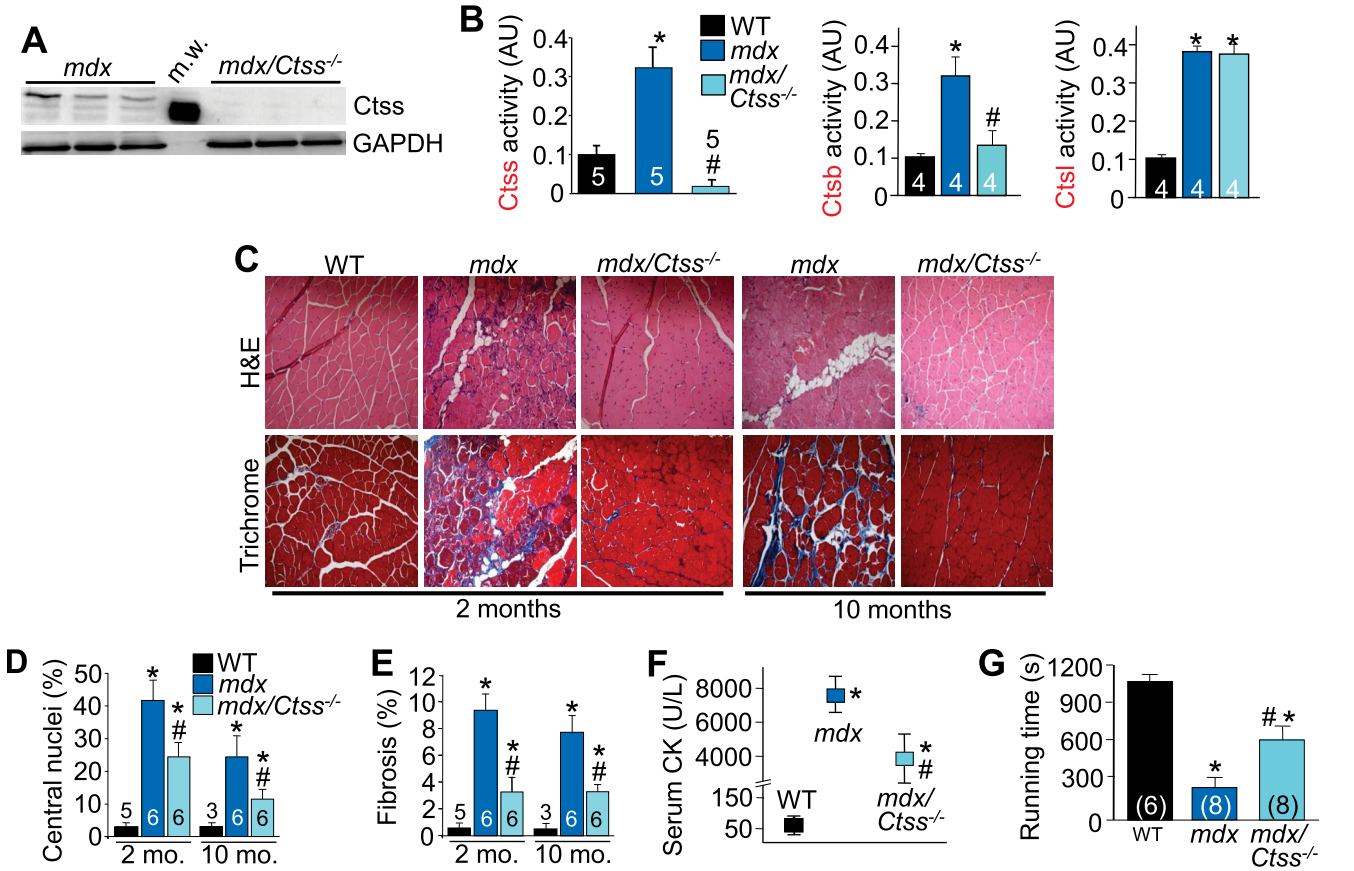

FIGURE 2. **Loss of *Ctss* in *mdx* mice attenuates disease pathogenesis.** *A* and *B*, Western blotting analysis for Ctss protein (*A*) and Ctss, cathepsin B (*Ctsb*), and cathepsin L (*Ctsl*) activity (*B*) from the quadriceps of 2-month-old *mdx/Ctss*$^{-/-}$, WT, and *mdx* mice. *, $p < 0.05$ *versus* WT; #, $p < 0.05$ *versus mdx*. The number of mice analyzed is indicated in the graph. GAPDH was used as a processing and loading control in *A*. *m. w.*, molecular weight markers. *AU*, arbitrary units. *C*, representative H&E and Masson trichrome-stained histological sections from quadriceps of 2- and 10-month-old mice of the indicated genotypes. Magnification is ×200. The *blue areas* represent fibrosis in the trichrome-stained sections. *D* and *E*, quantitation of the percentage of myofibers with centrally localized nuclei (*D*) and fibrotic area (*E*) from histological sections of the quadriceps in the genotypes shown at 2 and 10 months (*mo*) of age. The number of mice analyzed is shown in the graphs. *, $p < 0.05$ *versus* WT; #, $p < 0.05$ *versus mdx*. *F*, serum CK levels from the indicated genotypes of mice at 2 months of age. *, $p < 0.05$ *versus* WT; #, $p < 0.05$ *versus mdx*. $n = 6$ for each of the three genotypes evaluated. *U/L*, units/liter. *G*, treadmill running endurance in the three indicated groups of mice at 3 months of age at 10 m/min speed. The number of mice used is shown in the graphs. *, $p < 0.05$ *versus* WT; #, $p < 0.05$ *versus mdx*. All *error bars* represent mean ± S.E.

between myofibers but not within lysosomes, as co-stained with Lamp-2 (Fig. 1*D*). This suggested that, in dystrophic muscle, Ctss was up-regulated and primarily localized to the extracellular compartment.

To assess whether up-regulation of Ctss is induced following acute muscle injury, 60 μl of 1.2% $BaCl_2$ solution was injected into the TA muscle of WT mice (24). Significant induction of Ctss proteolytic activity and protein expression was observed with initial expression 3 days post-injury that was sustained through day 6 (Fig. 1, *E* and *F*). Myogenin was used to show myofibers undergoing regeneration because of a successful injury response. Collectively, these results demonstrate that endogenous Ctss is up-regulated following acute injury to skeletal muscle and during chronic muscular dystrophy.

Loss of Ctss Expression in mdx Mice Mitigates Dystrophic Disease—Genetic deletion of *Ctss* in an atherosclerotic mouse background resulted in reduced disease progression either through modulation of the immune response or stabilization of ECM components (26, 27). To determine whether Ctss is an effector of chronic muscle disease, we crossed the viable and fertile *Ctss*$^{-/-}$ mouse with the *mdx* model. Basal characterization of skeletal muscle from *Ctss*$^{-/-}$ mice showed no morphology signs of disease or any observable alterations (data not shown). Western blotting analysis and Ctss activity assays confirmed the loss of Ctss protein expression and proteolytic activity in the skeletal muscle of *mdx/Ctss*$^{-/-}$ mice (Fig. 2, *A* and *B*). Genetic deletion of *Ctss* in *mdx* mice also blunted the increase in activity of the cysteine protease cathepsin B but not the increase in cathepsin L, both of which are also up-regulated in dystrophic skeletal muscle (Fig. 2*B*).

Histological assessment of skeletal muscle from 2-month-old *mdx/Ctss*$^{-/-}$ mice showed a noticeable reduction in myofiber necrosis, fibrosis, and other aspects of muscle histopathology compared with *mdx* mice (Fig. 2*C*). This early time point (2 months) is especially important because it corresponds to the first few cycles of myofiber degeneration-regeneration during DMD pathogenesis in mice. Improvements in muscle histopathology were also observed in older (10-month-old) *mdx/Ctss*$^{-/-}$ mice (Fig. 2*C*). Furthermore, histological analysis of the diaphragms from *mdx/Ctss*$^{-/-}$ mice showed noticeably healthier tissue at both 2 and 10 months of age compared with *mdx* alone (data not shown). Quantitative assessment of the tissue histopathology and general muscle disease features also showed significant improvements in *mdx* mice with deletion

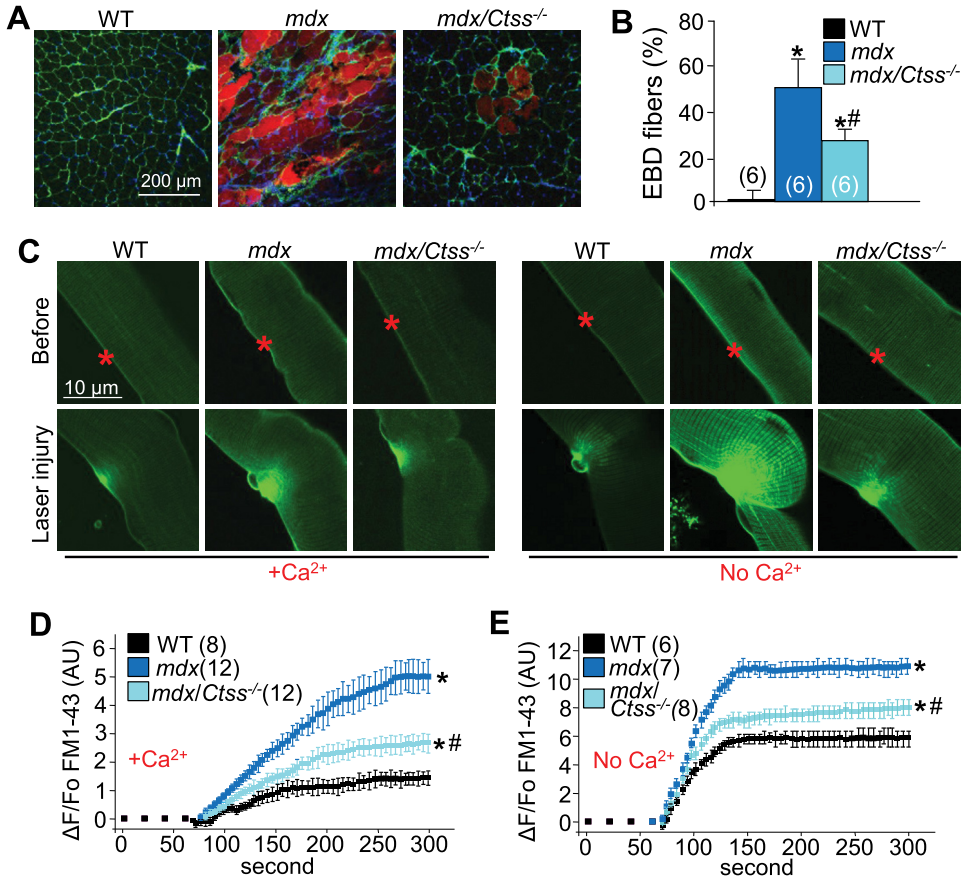

FIGURE 3. **Loss of *Ctss* in *mdx* muscle protects against sarcolemma membrane damage**. *A* and *B*, representative histological images (*A*) and quantitation of EBD uptake (*B*) in myofibers of the TA muscle in the indicated genotypes of mice. Wheat germ agglutinin-FITC (*green*) was used as a membrane marker. EBD-containing fibers fluoresce *red* under the imaging conditions used. The number of mice used is shown in the graph. *, $p < 0.05$ *versus* WT; #, $p < 0.05$ *versus mdx*. *C*, representative images for FM1-43 dye entry (*green*) from individually isolated flexor digitorum brevis myofibers from the indicated genotypes of mice. The fibers in the *top row* were uninjured, whereas those in the *bottom row* were laser-injured in the presence of 1.25 mM calcium (*left panel*) or absence of extracellular calcium (*right panel*). The *asterisks* show the area that will be injured with the laser. *D* and *E*, quantitative traces of FM1-43 dye entry after laser injury in the presence (*D*) or absence (*E*) of calcium as shown in *C* from six or more fibers for each mouse and a total of five separate animals for each genotype shown. *, $p < 0.05$ *versus* WT; #, $p < 0.05$ *versus mdx*. All *error bars* represent mean ± S.E. *AU*, arbitrary units.

of the *Ctss* gene. For example, central nucleation, tissue fibrosis, and serum creatine kinase (CK) levels were all significantly reduced in *mdx/Ctss*$^{-/-}$ mice compared with *mdx* mice alone (Fig. 2, *D–F*). This improvement in muscle histopathology and reduction in serum CK levels also correlated with improved muscle function because *mdx/Ctss*$^{-/-}$ mice performed significantly better than *mdx* mice when subjected to forced treadmill running at 3 months of age (Fig. 2*G*). Collectively, these results indicate that deletion of the *Ctss* gene improves muscle structure and function in dystrophic *mdx* mice.

To examine the potential mechanisms whereby loss of the *Ctss* gene might protect skeletal muscle in the *mdx* genetic background, we further interrogated sarcolemmal stability, given the significant reduction in total serum CK levels observed in the double genetically modified mice, which typically indicates levels of ongoing membrane rupture. Here we injected EBD intraperitoneally and subjected the mice to downhill running on a treadmill to increase the stress on myofiber membranes. Remarkably, significantly fewer EBD-positive myofibers (autofluoresces red) were observed in the skeletal muscle of *mdx/Ctss*$^{-/-}$ mice compared with *mdx*, suggesting decreased membrane rupture and increased membrane stability with *Ctss* deletion (Fig. 3, *A* and *B*).

To more directly evaluate sarcolemma membrane integrity at the single myofiber level, we measured the capacity of myofibers to be injured and/or reseal following direct laser injury to the sarcolemma, measured by influx of the membrane-impermeant dye FM1-43. Consistent with the known decrease in membrane stability of *mdx* myofibers, significantly greater FM1-43 fluorescence (*green*) was observed following acute laser membrane injury in myofibers from these mice (Fig. 3, *C* and *D*). However, less FM1-43 dye entry was observed in the myofibers isolated from the *mdx/Ctss*$^{-/-}$ skeletal muscle, further confirming that loss of Ctss protects against sarcolemma membrane damage in the dystrophic background (Fig. 3, *C* and *D*). To dissect whether deletion of *Ctss* primarily affects sarcolemma membrane stability or its resealing capacity, we repeated the assay in the absence of extracellular calcium (membrane resealing is a calcium-dependent process). Removal of calcium resulted in greater FM1-43 dye entry in the myofibers from all genotypes (Fig. 3, *C* and *E*), but the level of influx in the *mdx* background was still much greater, and this greater value was significantly reduced by deletion of the *Ctss* gene (Fig. 3*E*).

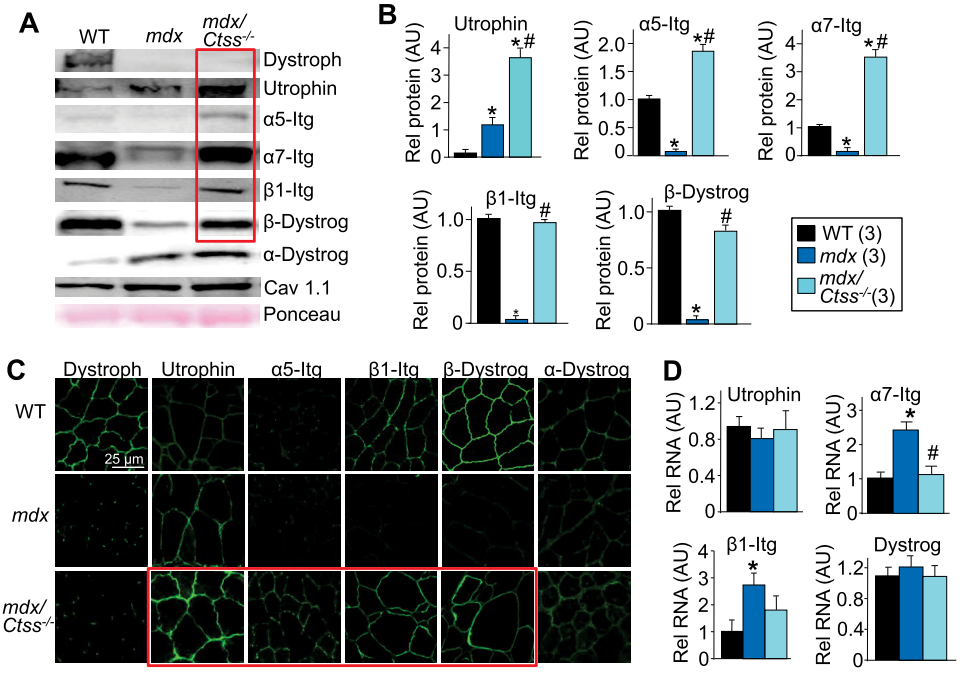

FIGURE 4. **Loss of Ctss in the muscle of *mdx* mice stabilizes and restores the abundance of sarcolemma adhesion complex proteins.** *A*, Western blotting of membrane protein extracts isolated from the quadriceps muscle of the indicated genotypes of mice at 2–3 months of age for the indicated proteins. Cav1.1 expression and Ponceau staining were used as loading controls. The *red box* shows the critical proteins that were increased in expression by loss of Ctss. *Dystroph*, dystrophin; *Itg*, integrin; *Dystrog*, dystroglycan; *Cav1.1*, L-type calcium channel. *B*, quantitative protein analysis for the indicated proteins in the quadriceps of the indicated genotypes of mice. A total of three separate animals and protein preparations was used for densitometric analysis.*, $p < 0.05$ *versus* WT; #, $p < 0.05$ *versus mdx*. All *error bars* represent mean ± S.E. *Rel*, relative. *AU*, arbitrary units. *C*, immunohistochemistry of the indicated proteins (*green*) from transverse histological sections of quadriceps of WT, *mdx*, and *mdx/Ctss*$^{-/-}$ mice. The *red box* shows the proteins that are stabilized and increase in expression in the absence of Ctss. *D*, quantitative PCR analysis for relative mRNA expression levels of the indicated genes from the quadriceps of the indicated mice at 2–3 months of age. *Error bars* represent mean ± S.E. ($n = 3$ mice each). *, $p < 0.05$ *versus* WT.

Hence, loss of *Ctss* does not directly affect membrane resealing but, instead, regulates the inherent stability of the membrane.

Increased protection against sarcolemma damage in *mdx/Ctss*$^{-/-}$ myofibers could be associated with restoration or increased abundance of sarcolemma adhesion protein components. More importantly, proteases are known to target and cleave individual proteins within the dystrophin-glycoprotein complex and utrophin/integrin complexes (28–31). Analysis of these component proteins that stabilize the membrane in membrane-enriched protein preparations showed that *mdx* muscle had reduced levels of β-dystroglycan, α5-integrin, α7-integrin, and β1-integrin, with a mild compensatory increase in utrophin (Fig. 4, *A* and *B*). Deletion of the *Ctss* gene in the *mdx* background restored the levels of each of these proteins within the sarcolemma and even promoted a greater increase in utrophin levels (Fig. 4, *A* and *B*). Confocal imaging analysis of histological sections from skeletal muscle for membrane localization of each of these proteins also showed a noticeable increase in the levels of β-dystroglycan, α5-integrin, α7-integrin, β1-integrin, and utrophin in *mdx/Ctss*$^{-/-}$ mice *versus mdx* (Fig. 4*C*). Up-regulation of utrophin partially compensates for the loss of dystrophin in the *mdx* mouse to augment sarcolemma stability (32). To show that the observed changes were due to alterations in protein stability, we also measured mRNA levels for these genes from skeletal muscle. The results show that, although mRNA levels for utrophin and the dystroglycan gene were unchanged, α7-integrin and β1-integrin were actually increased in muscle of *mdx* mice (Fig. 4*D*), although this increase is opposite of the observed decrease in protein. This result suggests that Ctss primarily affects protein levels and stability but not gene transcription or mRNA stability of the key membrane-stabilizing complexes. Collectively, these data indicate that genetic deletion of *Ctss* reduces the degradation of the sarcolemma adhesion components in skeletal muscle of *mdx* mice, thereby increasing membrane stability.

Ctss Overexpression Induces a Dystrophy-like Phenotype in Skeletal Muscle of Mice—Because Ctss is induced in both human DMD and mouse models of muscular dystrophy, we attempted to model this increase by creating skeletal muscle-specific transgenic mice with increased Ctss expression. Ctss TG mice were generated in the FVBN genetic background using a modified human skeletal α-actin promoter (Fig. 5*A*). Western blotting analysis for Ctss protein expression in skeletal muscle defined two different TG lines with higher or lower protein expression (Fig. 5*B*). All of the experiments presented here were performed in the higher TG-line1, although similar phenotypes with less pathology were observed in TG-line2 (data not shown). Ctss transgene expression was uniform in multiple skeletal muscles that are predominantly fast-twitch, although lower levels of expression were observed in the soleus with its greater slow fiber content, whereas the heart showed no expression (Fig. 5*C*). Ctss activity assays also showed significantly higher levels in skeletal muscle from Ctss TG mice (Fig. 5*D*), which was similar to the observed increase in Ctss activity in *mdx* skeletal muscle (Fig. 1*B*). Immunohistochemistry also showed that the majority of overexpressed Ctss localized to the

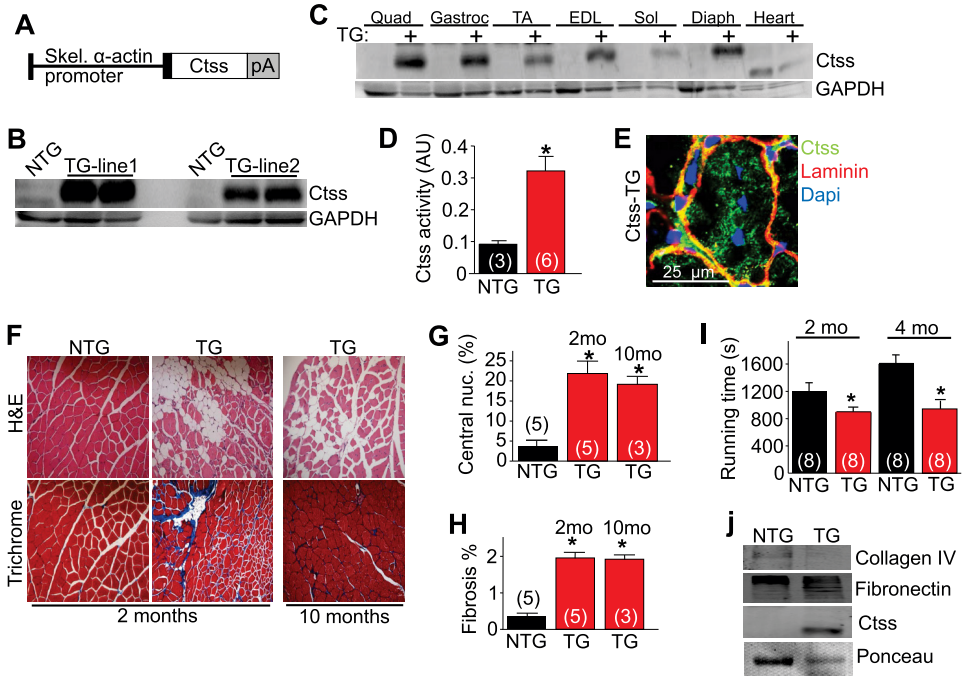

FIGURE 5. **Overexpression of Ctss in skeletal muscle produces a dystrophy-like phenotype.** *A*, schematic of the Ctss transgene construct used to make mice, directed by the skeletal (*Skel*) α-actin promoter. *pA* is the polyadenylation sequence. *B*, Western blotting analysis of Ctss and GAPDH expression from the quadriceps muscle of two separate transgenic founder lines at 2 months of age. *C*, Western blotting for Ctss expression in the different skeletal muscles shown, as well as heart from TG line 1, compared with control non-transgenic samples between each TG sample. GAPDH was a loading and processing control. *Quad*, quadriceps; *Gastroc*, gastrocnemius; *EDL*, extensor digitorum longus; *Sol*, soleus; *Diaph*, diaphragm. *D*, Ctss protease activity assay from the quadriceps muscle of NTG and Ctss TG mice. *, $p < 0.05$ *versus* NTG. The number of mice used is shown in the graph. *AU*, arbitrary units. *E*, immunohistochemistry from the quadriceps of Ctss TG mice for Ctss expression (*green*) *versus* the myofiber outline with laminin staining (*red*). Nuclei are shown in *blue* with DAPI staining. *F*, representative H&E and Masson trichrome histological sections from quadriceps of NTG and TG mice at the indicated ages. Magnification is ×200. *G* and *H*, quantitation of the percentage of myofibers with centrally localized nuclei (*nuc*) and fibrotic area in histological sections from quadriceps in the indicated genotypes of mice at 2 and 10 months of age. *, $p < 0.05$ *versus* NTG. The number of mice used is shown in the graph. *I*, treadmill running time for NTG and TG mice at the indicated 2 or 4 months of age, measured at 10 m/min speed. *, $p < 0.05$ *versus* NTG. *J*, Western blotting analysis of an enriched extracellular protein fraction from the quadriceps of NTG or TG mice for the indicated proteins. Ponceau was a loading control. All *error bars* represent mean ± S.E.

edges of the myofibers in the ECM region (Fig. 5*E*), similar to what was observed for endogenous Ctss in muscle from *mdx* mice (Fig. 1*D*). However, Ctss TG mice also showed some protein expression within the myofibers, likely as part of the secretory pathway within vesicles, which we did not readily observe in *mdx* muscle (Fig. 5*E* and "Discussion").

Histological analysis of skeletal muscle from Ctss TG mice showed disease at 2 months of age, characterized by accumulation of central nuclei in presumed regenerating myofibers, fatty tissue replacement, and fibrosis, all features of muscular dystrophy (Fig. 5, *F–H*). A similar tissue histopathology with increased quantitative indexes of disease was observed in skeletal muscle from Ctss TG mice at 10 months of age (Fig. 5, *F–H*). These pathogenic changes in skeletal muscle also correlated with a loss of skeletal muscle functional performance assessed by treadmill running at both 2 and 4 months of age (Fig. 5*I*). Finally, consistent with the proposed mechanism whereby increased Ctss expression and activity in dystrophic muscle might be degrading dystrophin-glycoprotein complex or ECM components, we observed increased degradation of collagen IV and fibronectin in ECM protein preparations from skeletal muscle of Ctss TG mice (Fig. 5*J*). Taken together, these results suggest that increased Ctss expression and activity in skeletal muscle is pathologic and, hence, could be the target for inhibition during muscular dystrophy as a novel therapeutic approach.

Discussion

Our study provides the first genetic evidence that elevated Ctss proteolytic activity in skeletal muscle is pathological and contributes to muscular dystrophy. Indeed, genetic deletion of *Ctss* in the skeletal muscle of *mdx* mice protected muscle from dystrophic disease, as shown by increased running endurance and blunted muscle histopathology as well as reduced serum CK levels. Broadly acting protease inhibition in muscular dystrophy achieved with either genetic modification or pharmacological inhibition has reduced muscular dystrophy manifestations in mouse models of this disease (15, 16, 33). However, an early pilot study testing the efficacy of Bestatin and Loxistatin, both of which are general inhibitors for multiple cathepsin family members, showed improved muscle function in infant DMD patients, but the effects were not reproduced in juvenile patients (34). This negative result might be explained by the lack of specificity and harmful off-target effects of these agents (35, 36).

A small compound, *N*-morpholinourea-leucine-homophenylalanine-vinyl-sulfonephenol (LHVS), is a more specific Ctss inhibitor with an IC_{50} of 5 nM (10, 11). *In vitro* and *in vivo* studies using LHVS have shown promising therapeutic effects such as decreased ECM remodeling in hypertension-induced heart failure (37) and increased neuroprotection following traumatic brain injury (38) or peripheral nerve trauma (39, 40).

These results confirm the specificity and efficacy of LHVS in targeting Ctss for a biologic effect *in vivo* that is consistent with its presumed function. Our results in *Ctss*$^{-/-}$ mice also suggest that a Ctss-specific inhibitor could be an interesting new strategy to treat DMD with potentially fewer side effects or undesirable off-target effects. Another interesting concept is that Ctss is somewhat unique in its ability to function outside of the lysosome, at neutral pH. Hence, Ctss might preferentially contribute to pathogenic events in muscular dystrophy compared with other proteases.

Human genetic studies have shown that the primary cause of muscular dystrophy is a loss of one of a myriad of genes that can directly or indirectly affect the structural integrity of the sarcolemma (4, 5). Activation of proteases in damaged muscle further diminishes the stability of the sarcolemma because of aberrant cleavage of other membrane adhesion complex proteins such as β-dystroglycan and integrins (28–31). For example, upregulation of integrin mRNA expression in the muscle of *mdx* mice (Fig. 4*D*) did not produce increased protein expression and localization in the sarcolemma membrane (Fig. 4, *A*–*C*), suggesting a continuous proteolysis of the integrin subunits in damaged *mdx* muscle, to which Ctss may contribute. Restoration and increased protein expression and localization of these sarcolemma adhesion components greatly enhance and protect the sarcolemma against contraction/exercise-induced injury (41). Thus, the improved sarcolemma stability of myofibers from *mdx/Ctss*$^{-/-}$ mice is likely because of increased abundance and stability of utrophin, β-dystroglycan, and integrin subunits (α5, α7, and β1) within this membrane (Fig. 4, *A*–*C*).

We also generated Ctss TG mice that exhibited comparable expression and proteolytic activity of Ctss to that normally induced in the skeletal muscle of *mdx* mice. Ctss TG mice showed a dystrophy-like disease pathology associated with muscle dysfunction and tissue histopathology. However, in addition to the extracellular expression of Ctss as normally observed for endogenous Ctss in *mdx* muscle, we observed intracellular Ctss protein expression within the myofibers of the TG mice, which is of unknown specificity and, hence, could potentially promote an artifactual mechanism whereby this protease cleaves important membrane-stabilizing proteins from within the vesicular compartment and membrane-trafficking network (Fig. 5*E*). Although this is a possibility, clearly endogenous Ctss that is induced with disease also traverses the intracellular vesicular trafficking network on its way to being secreted, where it could also have pathologic effects on these same membrane-stabilizing protein components. Hence we believe that the Ctss TG model still provides important information that is consistent with the observations in *Ctss*$^{-/-}$ *mdx* mice as well as with previous studies that showed some degree of protection from muscular dystrophy with pharmacologic protease inhibitors. Thus, moving forward, it will be important to determine how central Ctss is *versus* other induced proteases that are known to be induced in dystrophic skeletal muscle (although only Ctss might be secreted and active outside of the myofibers compared with other cathepsins that only function at a low pH). Such knowledge will help inform the best pharmacologic strategy and how one might want to design a drug to block Ctss *versus* other related and potentially pathogenic proteases of the same class or even of other classes. Despite this argument, our results suggest that Ctss is a critical protease and perhaps a highly specific inhibitor that blocks just this enzyme would be an ideal starting point for future studies with possible translation to the clinic.

Author Contributions—A. T. conducted most of the experiments, analyzed the results, and wrote the paper with M. M. and J. D. M. T. G. S. conducted the Western blotting and extraction of extracellular protein fractionation. M. A. S., D. V., O. K., V. P., and S. C. J. L. provided technical assistance. M. M. wrote the paper with A. T. and J. D. M. The study was conceived by J. D. M., who also oversaw all experimentation and interpretation of results.

References

1. Stark, A. E. (2015) Determinants of the incidence of Duchenne muscular dystrophy. *Ann. Transl. Med.* **3,** 287
2. Bushby, K., Finkel, R., Birnkrant, D. J., Case, L. E., Clemens, P. R., Cripe, L., Kaul, A., Kinnett, K., McDonald, C., Pandya, S., Poysky, J., Shapiro, F., Tomezsko, J., Constantin, C., and DMD Care Considerations Working Group (2010) Diagnosis and management of Duchenne muscular dystrophy, part 2: implementation of multidisciplinary care. *Lancet Neurol.* **9,** 177–189
3. Bushby, K., Finkel, R., Birnkrant, D. J., Case, L. E., Clemens, P. R., Cripe, L., Kaul, A., Kinnett, K., McDonald, C., Pandya, S., Poysky, J., Shapiro, F., Tomezsko, J., Constantin, C., and DMD Care Considerations Working Group (2010) Diagnosis and management of Duchenne muscular dystrophy, part 1: diagnosis, and pharmacological and psychosocial management. *Lancet Neurol.* **9,** 77–93
4. Gumerson, J. D., and Michele, D. E. (2011) The dystrophin-glycoprotein complex in the prevention of muscle damage. *J. Biomed. Biotechnol.* **2011,** 210797
5. Lapidos, K. A., Kakkar, R., and McNally, E. M. (2004) The dystrophin glycoprotein complex: signaling strength and integrity for the sarcolemma. *Circ. Res.* **94,** 1023–1031
6. Wein, N., Alfano, L., and Flanigan, K. M. (2015) Genetics and emerging treatments for Duchenne and Becker muscular dystrophy. *Pediatr. Clin. North Am.* **62,** 723–742
7. Hollinger, K., and Selsby, J. T. (2013) The physiological response of protease inhibition in dystrophic muscle. *Acta Physiol. (Oxf.)* **208,** 234–244
8. Mantle, D., and Preedy, V. R. (2002) Adverse and beneficial functions of proteolytic enzymes in skeletal muscle: an overview. *Adverse Drug React. Toxicol. Rev.* **21,** 31–49
9. Shi, G. P., Villadangos, J. A., Dranoff, G., Small, C., Gu, L., Haley, K. J., Riese, R., Ploegh, H. L., and Chapman, H. A. (1999) Cathepsin S required for normal MHC class II peptide loading and germinal center development. *Immunity* **10,** 197–206
10. Riese, R. J., Wolf, P. R., Brömme, D., Natkin, L. R., Villadangos, J. A., Ploegh, H. L., and Chapman, H. A. (1996) Essential role for cathepsin S in MHC class II-associated invariant chain processing and peptide loading. *Immunity* **4,** 357–366
11. Pierre, P., and Mellman, I. (1998) Developmental regulation of invariant chain proteolysis controls MHC class II trafficking in mouse dendritic cells. *Cell* **93,** 1135–1145
12. Conus, S., and Simon, H. U. (2010) Cathepsins and their involvement in immune responses. *Swiss Med. Wkly.* **140,** w13042
13. Bromme, D., and Wilson, S. (2011) in *Extracellular Matrix Degradation* (Parks, W. C., and Mecham, R. P., eds.), 1st ed., Springer, Berlin
14. Li, H., Mittal, A., Makonchuk, D. Y., Bhatnagar, S., and Kumar, A. (2009) Matrix metalloproteinase-9 inhibition ameliorates pathogenesis and improves skeletal muscle regeneration in muscular dystrophy. *Hum. Mol. Genet.* **18,** 2584–2598
15. Tjondrokoesoemo, A., Schips, T., Kanisicak, O., Sargent, M. A., and Molkentin, J. D. (2016) Genetic overexpression of Serpina3n attenuates muscular dystrophy in mice. *Hum. Mol. Genet.* **25,** 1192–1202

16. Morris, C. A., Selsby, J. T., Morris, L. D., Pendrak, K., and Sweeney, H. L. (2010) Bowman-Birk inhibitor attenuates dystrophic pathology in *mdx* mice. *J. Appl. Physiol.* **109,** 1492–1499
17. Baron, D., Magot, A., Ramstein, G., Steenman, M., Fayet, G., Chevalier, C., Jourdon, P., Houlgatte, R., Savagner, F., and Pereon, Y. (2011) Immune response and mitochondrial metabolism are commonly deregulated in DMD and aging skeletal muscle. *PloS ONE* **6,** e26952
18. Fang, J., Shi, G. P., and Vaghy, P. L. (2000) Identification of the increased expression of monocyte chemoattractant protein-1, cathepsin S, UPIX-1, and other genes in dystrophin-deficient mouse muscles by suppression subtractive hybridization. *J. Cell Biochem.* **79,** 164–172
19. Marotta, M., Ruiz-Roig, C., Sarria, Y., Peiro, J. L., Nuñez, F., Ceron, J., Munell, F., and Roig-Quilis, M. (2009) Muscle genome-wide expression profiling during disease evolution in *mdx* mice. *Physiol. Genomics* **37,** 119–132
20. Shin, J. H., Hakim, C. H., Zhang, K., and Duan, D. (2011) Genotyping mdx, mdx3cv, and mdx4cv mice by primer competition polymerase chain reaction. *Muscle Nerve* **43,** 283–286
21. Brennan, K. J., and Hardeman, E. C. (1993) Quantitative analysis of the human α-skeletal actin gene in transgenic mice. *J. Biol. Chem.* **268,** 719–725
22. Kobayashi, Y. M., Rader, E. P., Crawford, R. W., Iyengar, N. K., Thedens, D. R., Faulkner, J. A., Parikh, S. V., Weiss, R. M., Chamberlain, J. S., Moore, S. A., and Campbell, K. P. (2008) Sarcolemma-localized nNOS is required to maintain activity after mild exercise. *Nature* **456,** 511–515
23. Barallobre-Barreiro, J., Didangelos, A., Yin, X., Doménech, N., and Mayr, M. (2013) A sequential extraction methodology for cardiac extracellular matrix prior to proteomics analysis. *Methods Mol. Biol.* **1005,** 215–223
24. Casar, J. C., Cabello-Verrugio, C., Olguin, H., Aldunate, R., Inestrosa, N. C., and Brandan, E. (2004) Heparan sulfate proteoglycans are increased during skeletal muscle regeneration: requirement of syndecan-3 for successful fiber formation. *J. Cell Sci.* **117,** 73–84
25. Millay, D. P., Goonasekera, S. A., Sargent, M. A., Maillet, M., Aronow, B. J., and Molkentin, J. D. (2009) Calcium influx is sufficient to induce muscular dystrophy through a TRPC-dependent mechanism. *Proc. Natl. Acad. Sci. U.S.A.* **106,** 19023–19028
26. de Nooijer, R., Bot, I., von der Thüsen, J. H., Leeuwenburgh, M. A., Overkleeft, H. S., Kraaijeveld, A. O., Dorland, R., van Santbrink, P. J., van Heiningen, S. H., Westra, M. M., Kovanen, P. T., Jukema, J. W., van der Wall, E. E., van Berkel, T. J., Shi, G. P., and Biessen, E. A. (2009) Leukocyte cathepsin S is a potent regulator of both cell and matrix turnover in advanced atherosclerosis. *Arterioscler. Thromb. Vasc. Biol.* **29,** 188–194
27. Sukhova, G. K., Zhang, Y., Pan, J. H., Wada, Y., Yamamoto, T., Naito, M., Kodama, T., Tsimikas, S., Witztum, J. L., Lu, M. L., Sakara, Y., Chin, M. T., Libby, P., and Shi, G. P. (2003) Deficiency of cathepsin S reduces atherosclerosis in LDL receptor-deficient mice. *J. Clin. Invest.* **111,** 897–906
28. Liu, J., Gurpur, P. B., and Kaufman, S. J. (2008) Genetically determined proteolytic cleavage modulates $\alpha7\beta1$ integrin function. *J. Biol. Chem.* **283,** 35668–35678
29. Badorff, C., Lee, G. H., Lamphear, B. J., Martone, M. E., Campbell, K. P., Rhoads, R. E., and Knowlton, K. U. (1999) Enteroviral protease 2A cleaves dystrophin: evidence of cytoskeletal disruption in an acquired cardiomyopathy. *Nat. Med.* **5,** 320–326
30. Earnest, J. P., Santos, G. F., Zuerbig, S., and Fox, J. E. (1995) Dystrophin-related protein in the platelet membrane skeleton: integrin-induced change in detergent-insolubility and cleavage by calpain in aggregating platelets. *J. Biol. Chem.* **270,** 27259–27265
31. Kramerova, I., Kudryashova, E., Wu, B., and Spencer, M. J. (2006) Regulation of the M-cadherin-β-catenin complex by calpain 3 during terminal stages of myogenic differentiation. *Mol. Cell Biol.* **26,** 8437–8447
32. Blake, D. J., Tinsley, J. M., and Davies, K. E. (1996) Utrophin: a structural and functional comparison to dystrophin. *Brain Pathol.* **6,** 37–47
33. Sawada, H., Nagahiro, K., Kikukawa, Y., Ban, S., Kakefuda, R., Shiomi, T., and Yokosawa, H. (2003) Therapeutic effect of camostat mesilate on Duchenne muscular dystrophy in *mdx* mice. *Biol. Pharm. Bull.* **26,** 1025–1027
34. Satoyoshi, E. (1992) Therapeutic trials on progressive muscular dystrophy. *Intern. Med.* **31,** 841–846
35. Suzuki, H., Caughey, G. H., Gao, X. P., and Rubinstein, I. (1998) Mast cell chymase-like protease (s) modulates *Escherichia coli* lipopolysaccharide-induced vasomotor dysfunction in skeletal muscle *in vivo*. *J. Pharmacol. Exp. Ther.* **284,** 1156–1164
36. Fukushima, K., Arai, M., Kohno, Y., Suwa, T., and Satoh, T. (1990) An epoxysuccinic acid derivative(loxistatin)-induced hepatic injury in rats and hamsters. *Toxicol. Appl. Pharmacol.* **105,** 1–12
37. Cheng, X. W., Obata, K., Kuzuya, M., Izawa, H., Nakamura, K., Asai, E., Nagasaka, T., Saka, M., Kimata, T., Noda, A., Nagata, K., Jin, H., Shi, G. P., Iguchi, A., Murohara, T., and Yokota, M. (2006) Elastolytic cathepsin induction/activation system exists in myocardium and is upregulated in hypertensive heart failure. *Hypertension* **48,** 979–987
38. Xu, J., Wang, H., Ding, K., Lu, X., Li, T., Wang, J., Wang, C., and Wang, J. (2013) Inhibition of cathepsin S produces neuroprotective effects after traumatic brain injury in mice. *Mediators Inflamm.* **2013,** 187873
39. Barclay, J., Clark, A. K., Ganju, P., Gentry, C., Patel, S., Wotherspoon, G., Buxton, F., Song, C., Ullah, J., Winter, J., Fox, A., Bevan, S., and Malcangio, M. (2007) Role of the cysteine protease cathepsin S in neuropathic hyperalgesia. *Pain* **130,** 225–234
40. Clark, A. K., Yip, P. K., Grist, J., Gentry, C., Staniland, A. A., Marchand, F., Dehvari, M., Wotherspoon, G., Winter, J., Ullah, J., Bevan, S., and Malcangio, M. (2007) Inhibition of spinal microglial cathepsin S for the reversal of neuropathic pain. *Proc. Natl. Acad. Sci. U.S.A.* **104,** 10655–10660
41. Han, R., Kanagawa, M., Yoshida-Moriguchi, T., Rader, E. P., Ng, R. A., Michele, D. E., Muirhead, D. E., Kunz, S., Moore, S. A., Iannaccone, S. T., Miyake, K., McNeil, P. L., Mayer, U., Oldstone, M. B., Faulkner, J. A., and Campbell, K. P. (2009) Basal lamina strengthens cell membrane integrity via the laminin G domain-binding motif of α-dystroglycan. *Proc. Natl. Acad. Sci. U.S.A.* **106,** 12573–12579